Geophysical Research Letters®

RESEARCH LETTER
10.1029/2021GL092632

3D Deep Electrical Resistivity Tomography of the Lusi Eruption Site in East Java

Adriano Mazzini[1,2], Aurore Carrier[3], Alessandra Sciarra[2,4], Federico Fischanger[5], Anton Winarto-Putro[6], and Matteo Lupi[3]

[1]Centre for Earth Evolution and Dynamics (CEED), University of Oslo, Oslo, Norway, [2]Istituto Nazionale di Geofisica e Vulcanologia, Rome, Italy, [3]Department of Earth Sciences, University of Geneva, Geneva, Switzerland, [4]Consiglio Nazionale delle Ricerche - Istituto di Geologia Ambientale e Geoingegneria, (CNR-IGAG), Rome, Italy, [5]Geostudi Astier srl, Livorno, Italy, [6]Pusat Pengendalian Lumpur Sidoarjo (PPLS), Sidoarjo, Indonesia

Key Points:

- An extensive 3D deep electrical resistivity tomography survey was performed at the Lusi mud eruption, Indonesia, over a region of 15 km^2
- The low resistivity area with active vents and ongoing subsidence (600 × 100 m) is mapped narrowing in size up to 500 m below the surface
- The Lusi conduit has an ellipsoidal shape controlled by the Watukosek fault system through which upwell the deep-sourced fluids

Supporting Information:

Supporting Information may be found in the online version of this article.

Correspondence to:

A. Mazzini,
adriano.mazzini@geo.uio.no

Citation:

Mazzini, A., Carrier, A., Sciarra, A., Fischanger, F., Winarto-Putro, A., & Lupi, M. (2021). 3D deep electrical resistivity tomography of the Lusi eruption site in East Java. *Geophysical Research Letters*, *48*, e2021GL092632. https://doi.org/10.1029/2021GL092632

Received 26 JAN 2021
Accepted 26 AUG 2021

Abstract Lusi is a sediment-hosted geothermal system relentlessly erupting since May 2006 in the East Java back-arc sedimentary basin. Lusi provides the unprecedented opportunity to study the development of the early phases of a new-born piercement structure and its impact on society. In order to investigate the shallow plumbing system of this large-scale eruption, we deployed a pool of 25 IRIS V-Fullwavers to conduct a 3D deep electrical resistivity tomography extending over ~15 km^2 around the eruption site. The inverted data reveal the structure of the subsided area hosting the region where a mix of groundwater, mud breccia, hydrocarbons and boiling hydrothermal fluids are stored. Our investigation also points out the link between a well-developed fault system and the upwelling of the deep-seated fluids that initiated, and still drive, the development of the new-born Lusi eruption.

Plain Language Summary Lusi is the largest erupting clastic system on Earth and is active in the East Java back-arc sedimentary basin since May the 29th 2006. This spectacular system features a 200 m wide active crater zone surrounded by thousands of satellite seeps that extend over a region of 7 km^2. A wealth of geochemical, petrographical, geophysical, and modeling studies revealed that Lusi is connected at depth with the neighboring Arjuno-Welirang volcanic complex through a system of faults. However, the interaction of these tectonic structures with the shallow depth plumbing system remained so far unknown. Here we present the results of an extensive (15 km^2) 3D deep electrical resistivity tomography survey. Results reveal the subsurface morphology of this new-born eruption and disclose the link between a well-developed fault system and the upwelling of the deep-sourced fluids.

1. Introduction

Electrical resistivity and magnetotelluric are potential methods often used in hydrogeophysical and geothermal studies. Electrical resistivity tomography is traditionally a shallow-reaching method unless using logistically challenging configurations often prohibitive in urbanized areas. Magnetotelluric enables prospecting much greater depths but it is normally hampering resolution of the shallower data. Both methods are hindered by the electromagnetic noise that is typical of urbanized regions. Hence, the prospection of the upper kilometer of the crust with electrical methods is not trivial. However, Deep Electrical Resistivity Tomography (DERT) has been previously attempted and few successful data acquisition experiments were conducted over the last decade. Revil et al. (2011) investigated the hydrogeology of the Stromboli volcano in Southern Italy with several 2D roll-alongs of multi-core cables with 50 m electrode spacing. Balasco et al. (2011) and Pucci et al. (2016) used dipole-dipole and remote electrode configuration, respectively, to attain 2D profiles ~1,000 m deep to investigate seismogenic structures in the Italian Apennines. Experiments aiming to obtain large-scale 3D images have been attempted by Troiano et al. (2019) who provided a resistive image of the shallow hydrothermal system of the Campi Flegrei, Italy. Such type of studies became possible thanks to IRIS® instruments that released the Fullwaver system (Carrier et al., 2019; Lajaunie et al., 2019; Troiano et al., 2019) equipped with GPS-synchronised voltmeters that can be deployed to form a network even in urbanized areas. This hardware was initially conceived to investigate the chargeability and resistivity contrasts often encountered in ore deposits. However, Carrier et al. (2019) has shown that the Fullwaver technology could also be suitable to prospect middle-enthalpy geothermal environments. Moreover this versatile system can acquire large-scale 3D surveys on active geothermal structures where

complex plumbing systems remain undisclosed. The opportunity to investigate this type of features occurred in Indonesia in 2018.

In the East Java Basin is present the largest erupting clastic system on Earth, the LUmpur SIdoarjo, nicknamed Lusi. Lusi is a large sediment-hosted geothermal system that pierced on the Earth's surface the 29th of May 2006 along the Watukosek fault system (Mazzini et al., 2007, 2009; Van Noorden, 2006). This major crustal-scale tectonic discontinuity reaches the neighboring volcanic arc, to the SW of Lusi, and extends towards the NE of Java Island (Miller & Mazzini, 2018; Moscariello et al., 2018; Sciarra et al., 2018). The Quaternary volcanic deposits hinder the tracing of the Watukosek fault system across the volcanic arc but the alignment of the eruptive centers allowed Mazzini et al. (2012) and Lupi et al. (2018) to speculate that the Watukosek may actually be a regional-scale feature. Numerous scientific studies from different disciplines have shown that this eruption is connected and fed at depth by the neighboring volcanic complex (Fallahi et al., 2017; Inguaggiato et al., 2018; Zaputlyaeva et al., 2019). The migration of magmatic and hydrothermal fluids into the deep organic-rich source rock deposits of the basin, triggered thermometamorphic reactions and fluids overpressure at depth (Malvoisin et al., 2018; Mazzini et al., 2012; Svensen et al., 2018; Zaputlyaeva et al., 2020). These fluids are ultimately released at the Lusi crater with impressive geysering activity at the surface (Karyono et al., 2017; Lupi et al., 2018). This part of the island is also characterized by numerous diapirs and seismic profiles show that some of these have undergone eruption and subsidence (Istadi et al., 2009; Miller & Mazzini, 2018; Moscariello et al., 2018). Several geochemical (Inguaggiato et al., 2018; Mazzini et al., 2012, 2018; Sciarra et al., 2018; Zaputlyaeva et al., 2019), geological (Mazzini et al., 2021; Moscariello et al., 2018; Samankassou et al., 2018; Zaputlyaeva et al., 2020), numerical (Collignon, Schmid, et al., 2018; Lupi et al., 2013, 2014; Svensen et al., 2018) and geophysical (Karyono et al., 2017; Lupi et al., 2018; Mauri, Husein, Mazzini, Irawan, et al., 2018, Mauri, Husein, Mazzini, Karyono, et al., 2018; Panzera et al., 2018; Obermann et al., 2018; Osorio Riffo et al., 2021) studies contributed to the better understanding of the subsurface structure of Lusi. However, to date a clear picture of the Lusi shallow plumbing system is still missing. In order to explore the geometry of the structures below and around this active vent, we designed an electrical survey using a IRIS Fullwaver system. Here we describe the features obtained with this 3D DERT experiment revealing the geometries characterizing a vent system during its infancy.

2. Data Acquisition and Processing

The IRIS Fullwaver system is a quasi-cableless innovative technology that allows to handle electric noise issues typical of urbanized areas. The whole full-waveform acquisition at 100 Hz favors the removal of the noise during data processing. Furthermore, the high-power transmitters (between 5 and 10 kW) eases the prospection down to several hundred meters depth and the lack of multi-core cables allow a full 3D acquisition. Further details about this hardware are illustrated by Carrier et al. (2019) and Lajaunie et al. (2019).

This functional system was shipped to Surabaya in September 2018 to complete a full 3D survey of the area around the Lusi eruption site (Figure 1). The month of September was specifically selected as it was the end of the dry season thus allowing the access, and the deployment of the instruments, in areas that are typically flooded with mud. Lusi is a large eruption site visible from satellite images (Figure 1b). The area covered by the erupted mud breccia (term used to define a mixture of fine-grained sediments and rock clasts fragmented during the transport within the conduit, Mazzini & Etiope, 2017) extends over a surface of ~7 km^2 and it would certainly be even larger without the framing embankment built to contain the erupted mud and thus protect the surrounding settlements (Figure 1b). Lusi's activity occurs at two (and sometimes three) main active sub-circular vents whose size approximates 100 m in diameter (Di Felice et al., 2018; Di Stefano et al., 2018; Mazzini et al., 2021). This active region is surrounded by a ~600 m diameter sub-circular hydrothermal pond where the erupted mud is initially stocked (e.g., Di Felice et al., 2018; Di Stefano et al., 2018; Lupi et al., 2018).

The outskirts of this inaccessible pond become gradually drier until the area is walkable. In this accessible area we deployed our instruments and extended the deployment outside the embankment wall (Figure 1). We used a VIP 5000 transmitter. Our pool consisted in 25 V-Fullvawers (receiving nodes) and one I-Fullwavers (injection node) used to survey the ~15 km^2 area. We performed three *3D roll-alongs*. For each one

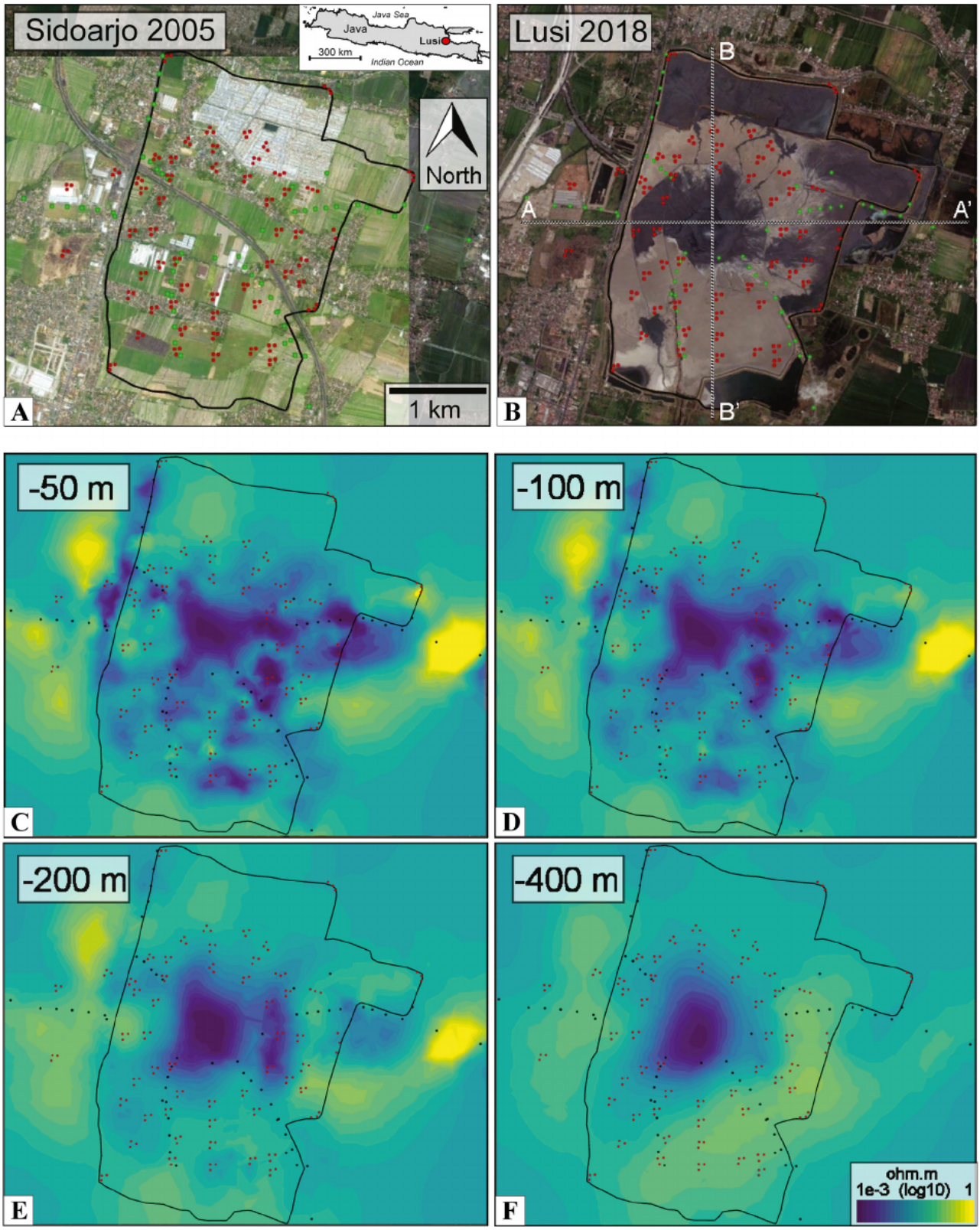

Figure 1.

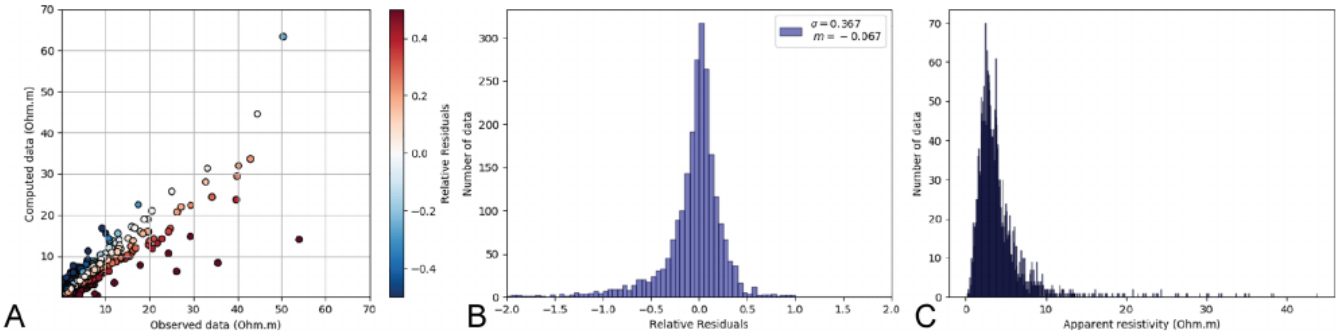

Figure 2. Data overview. (a) Cross-plot and (b) histogram. (c) Distribution of the apparent resistivity.

of them it was kept a minimum of 6 V-Fullwavers in place to grant continuity across acquisitions. Each V-Fullwaver handled two dipoles, that is, 3 electrodes deployed as shown in Figure 1 (red dots). The spacing between the M and N electrodes of each dipole was 50 m and deployed in a L configuration (unless logistically impossible). The injection electrodes A and B (green dots in Figure 1) were deployed along linear directions (when possible). The B electrode was maintained fix at one end and the A electrode moved away with intervals of ∼100 m. Using this technique we performed 84 injections. Lusi is a conductive environment and the contact resistance during acquisitions spanned from 20 to 720 Ohm and the injections of current ranged from 2 to 9.8 Amps. Each injection lasted approximately 300 s. This allowed the stacking of the signal to minimize the effect of electromagnetic noise and to compensate the extremely high conductivity of the prospected lithologies. The positions of the A, B, M, and N electrodes were surveyed with a high precision differential GNSS device, and all the points have an error smaller than 2 m. The topography was extracted from a high resolution DEM scan provided by the Pusat Pengendalian Lumpur Sidoarjo (PPLS), (the Indonesian Ministry agency supervising the mitigation infrastructures at the Lusi site).

To process the raw data stored in the V- and I- Fullwavers we used the *Full-wave viewer* software available at http://www.iris-instruments.com. The first step consisted in synchronizing eventually out of sync data (i.e., due to possible GPS unlocking of the V-Fullwaver). The following workflow included the filtering of the spikes and sudden changes of self-potential, the stacking of the data, calculating the average voltage across parts of the injection time on the stacked period, and finally computing the resistance from the measurements. We kept 3696 values of the total 82 × 25 × 2 theoretical points. The measuring points that were discarded had either non-stamped GPS or anomalous amplitudes. Note that the signal amplitude of the 3696 data spanned from 0.0001 to 21.4 mV. The data set had a standard deviation comprised between 0.03 and 46 mV. The data characterized either by a low signal (i.e., Vp ≤ 0.01 mV) or by a high standard deviation (i.e., ≥50%) were manually reprocessed. The data are shown in Figure 2. Next, *PROSYS* (http://www.iris-instruments.com) and *BERT* (https://gitlab.com/resistivity-net/bert) software were used for the post-processing. This reduced the initial 3696 data points to 2331 that have been used to perform the inversion. We used BERT to invert the data set (see Supporting Information S1) (Günther et al., 2006; Rücker et al., 2006). The inverted data set features signal amplitudes spanning from 0.2 to 21.4 mV with standard deviations from 0.03 to 4.5 mV. A detailed description of the forward modeling used in this experiment is presented in the Supporting Information S1. These results indicate that the distribution of the reception/transmission dipoles could reliably image the subsurface structures hosted in the conductive environment of Lusi.

Figure 1. Distribution of the 25 Fullwaver system in the Sidoarjo district, Java. (a) Aerial image of the region around Lusi before its inception (Credit Crisp, 2005). The area displays settlements and rice cultivation fields intersected by a large motorway. Inset map of Java Island. (b) The same area in 2018 (satellite image from Google Earth Pro) is covered by a thick (i.e., more than 10 m) cover of mud breccia erupted from the crater site. This information must be taken into account when interpreting the shallow region of the DERT inverted data (c.f., Figures (c–f)). The deployment of the V-Fullwaver around the eruption site is indicated with green (injection points) and red (receiving electrodes) dots. For comparison the same points are also plotted in panel (a) The A-A' and B-B' lines indicate the position of the cross sections shown in Figure 3. The intersection between these two profiles coincides broadly (as the vents are moving over the years) with the position of the active vents. The black line shows the contour of the embankment built to contain the erupted mud breccia and to protect the surrounding settlements. (c–f) Horizontal slices of the inverted 3D resistive model. The central region marked by low resistive values corresponds to the crater area surrounded by the hydrothermal pond from which depart multiple streams draining the crater area.

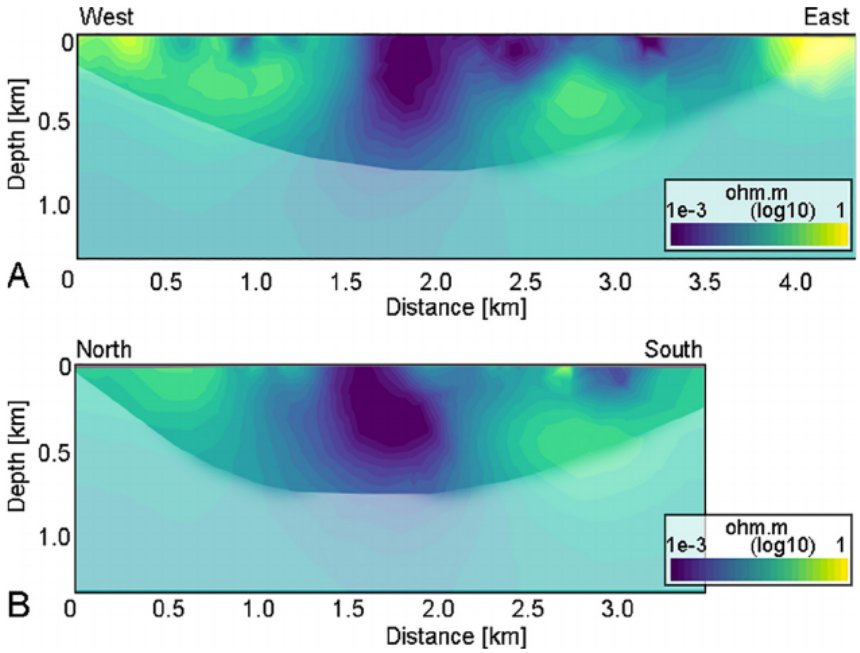

Figure 3. Cross sections of the inverted data set. The directions of the cross sections are shown in Figure 1b. Based on the coverage quantification (Figure S7) we shaded regions where interpretation of the results shall be handled with care.

3. Results and Discussion

3.1. A Fluid-Saturated Basin

The mud breccia erupted from Lusi is clay-dominated and saturated with highly conductive hydrocarbons. Similarly, the sedimentary basin hosting Lusi consists of clays and alternating clayey and sandy intervals for at least in the uppermost 2 km where the water table is found only few meters below the ground level. Despite this challenging highly conductive environment, the inverted resistivities span three orders of magnitude. The apparent resistivity of the data is extremely low (as expected) and ranges from 0.14 Ohm.m to 141 Ohm.m. The mean value is 4.23 Ohm.m and the standard deviation is 4.94 Ohm.m. Figures 1c–1f shows horizontal slices of the resistivity model obtained with the acquired data. By comparing Figure 1a with Figure 1c we notice that the lowest resistive values occur in regions used until 2006 as rice fields. Vice-versa, regions characterized by high resistivity inside Lusi's embankment correspond to buildings and anthropogenic constructions that are currently buried beneath the erupted mud breccia. The areas outside the embankment, where no erupted mud breccia is present, show higher resistivity values. A well-defined linear region with low values frames the western side of the embankment, where the railway is running. This is known to be a region of significant water infiltration (Figure 1a). The sensitivity tests and the forward modeling shown in the Supporting Information S1 reveal we attain good sensitivity in the region immediately below the surface of the active vents. This region (Figure 1b) is dominated by extremely low resistivity values (Figure 1c–1f). Figure 1f also shows that this high conductive zone has a sub elliptical funnel-like shape gradually decreasing in size at greater depths. The E-W oriented cross section shown in Figure 3a highlights that the region affected by low resistivity values is about 600 m wide. Across the perpendicular N-S direction (Figure 3b) this region extends up to 1,000 m. The lowest resistive values are found until about 500 m depth. In order to compare our newly acquired data with old resistivity logs collected before the Lusi inception, we inspected the profiles from the BJP-1 borehole (Lupi et al., 2014). Unfortunately, only less than 50 m of log (i.e., between 1,200-1,300 feet depth) is available for comparison with our data. In addition, as broadly documented, the survey area was exposed to extensive fracturing, subsidence, and fluids circulation through systems of fractures and seepage sites that mutated their position during more than 15 years of vigorous eruption (Lupi et al., 2018; Mauri, Husein, Mazzini, Irawan, et al., 2018; Mazzini et al., 2009, 2012, 2021; Moscariello et al., 2018; Obermann et al., 2018; Osorio Riffo et al., 2021; Panzera

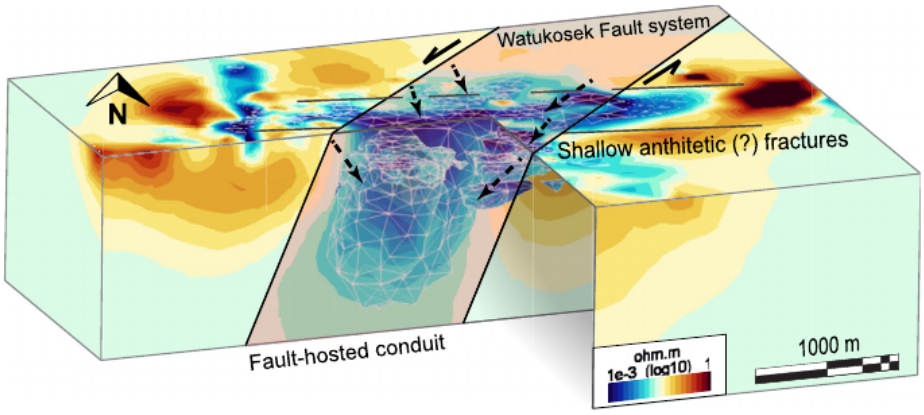

Figure 4. 3D projection of the acquired deep electrical resistivity tomography data. Extracted cells with resistivities below 2.5 Ohm.m underneath the active vents highlight the area of collapse (dashed black arrows). The red-shaded area indicates the Watukosek fault system that intersects Lusi.

et al., 2018; Sciarra et al., 2018; Zaputlyaeva et al., 2019). Therefore it would be impossible to compare the properties of this totally new environment with potential resistivity logs collected in pristine sedimentary deposits.

3.2. Ongoing Subsidence Around the Hydrothermal Pond

Piercement structures are typically characterized by gradual constant collapse ongoing around the vent area. This is visible for the large scale magmatic volcanoes with large-scale caldera collapse as well as for ancient hydrothermal vent structures and for mud volcanoes worldwide (e.g., Berndt et al., 2006; Collignon, Mazzini, et al., 2018; Deville et al., 2010; Dupuis et al., 2019; Kopf, 2008; Mazzini & Etiope, 2017; Mazzini et al., 2019; Planke et al., 2005; Svensen et al., 2006). The collapse observed with geophysical investigations from numerous piercements has also been related to potential shallow chambers that gather the overpressure of a deeper-rooted conduit and release it during the eruptions (e.g., Deville et al., 2003; Planke et al., 2003; Praeg et al., 2009). Likewise, the volume of the subsided area has also been used to infer the amounts of erupted sediments from these (at times buried) palaeo piercements sometimes displaying multiple staked eruptive events and collapse features (Dupuis et al., 2019; Kirkham et al., 2017).

It is challenging to establish the collapse rates of these structures precisely because most of the studies are conducted on palaeo systems whose precise ages are difficult to constrain. The Lusi eruption provides the opportunity to monitor the ongoing collapse of a hydrothermal vent during its early phases of evolution. Istadi et al. (2009) investigated with a GPS network the ongoing Lusi subsidence measuring vertical displacements up to 92 cm within the first month of activity. The authors also estimated that during the first 4 years of Lusi activity a collapse zone of more than 50 m would occur. The gradual subsidence in the area was also observed using InSAR data acquired during various periods (Aoki & Sidiq, 2014; Fukushima et al., 2009; Istadi et al., 2009; Rudolph et al., 2013; Shirzaei et al., 2015). Recent investigations targeted the Lusi shallow system inverting HVSR data (Panzera et al., 2018) or measuring the residual negative Bouguer anomalies (Mauri, Husein, Mazzini, Irawan, et al., 2018, Mauri, Husein, Mazzini, Karyono, et al., 2018; Osorio Riffo et al., 2021) suggesting a significant subsidence over a surface of several hundreds of meters in diameter. Our new geoelectrical data are consistent with previous investigations and allow refining more precisely the geometry of this subsiding area. We estimate that after 12 years of Lusi's inception, a collapse region of 0.6 km^2 developed around the active vents (Figure 3). From the 3D model, we isolated the cells below the active vent marked by resistivities below 2.5 Ohm.m and computed the volume (Figure 4). We therefore calculated a total volume of 0.17 km^3 that is associated with the remarkable collapse has been affecting the Lusi eruption site during the first 12 years of activity. Estimates accounting for the monitored flow rates of the Lusi eruption reveal that this system erupted 0.3 km^3 of mud breccia during the first 13 years of activity (Mazzini et al., 2021). This conservative estimate, accounts only for the flow rate measurements, however it is clear that a large area around the crater has been subsiding and filled with erupted material that remains

unaccounted in the above budget. Combining the flow rate data with our geoelectrical data, we estimate a total budget of 0.47 km^3 of mud breccia (i.e., including the erupted volume and that trapped in the collapse zone around the carter). These large volumes are comparable with those assessed for Touragay mud volcano (Alizadeh et al., 2016), the largest onshore mud volcano on Earth, and are similar to those of many others large scale structures of similar size. To put things further into prospective, the 2010 eruption of the Eyjafjallajökull volcano was estimated to have emitted about 0.3 km^3 of volcanic products (Gudmundsson et al., 2012). This emphasizes that Lusi is not just an erupting vent, but rather a large system competing in terms of volumes of subsidence rates and erupted solid/gas phases with geologically mature structures that featured several eruption cycles. This aspect has been emphasized by a recent study where is reported the amount of gas released by Lusi (Mazzini et al., 2021). The measurements reveal that Lusi emits CO_2 (0.35–0.78 Tg $year^{-1}$) in amounts comparable with that of magmatic volcanoes. In addition CH_4 emissions are estimated to be around 0.1 Tg $year^{-1}$, making Lusi the largest methane vent currently active on Earth.

Di Felice et al. (2018) used drone footages/videos and IR photogrammetry mosaics to reveal that the subcircular hydrothermal pond (~600 m in diameter) surrounding the vents is characterized by intense bubbling of boiling fluids throughout all its surface. Based on IR patterns of the mud, the authors also suggested that the focused expulsion of 100°C sediments and fluids from the central vent, trigger convective movements of the mud in the funnel-shaped subsurface of the pond. The recorded low resistivity measured in the area below the imaged hydrothermal pond (compare satellite image in Figures 1b and 1c–1f), are in agreement with the observed fluids- (water and gas) saturated mud at elevated (100°C) temperatures. Figures 1c–1f show that the resistivity progressively (yet slowly) increases with depth and the low values area gradually narrows. We interpret this as the bottom pinching of the funnel-shaped fractured subsiding region (i.e., hosted in the fault). Assuming that the shallow plumbing system of Lusi resembles to the conduit of a volcanic vent, Collignon, Schmid, et al. (2018) estimated that the radius of such conduit should not be larger than 1.5 m in order to match the maximal mud discharge recorded. Based on our new data, we propose that such a plumbing system may instead consist of a highly fractured region, hosted by the fault, where the active transport of fluids feeding Lusi takes place.

3.3. Intersecting the Watukosek Fault System

Horizontal and vertical DERT profiles provide important insights on the geometry of the Lusi plumbing system. The deepest horizontal slices (Figures 1e–1f) highlight that the low-resistive body stretches towards the SW forming a corridor with gradually increasing resistivity. The eastern flank of the low resistivity zone appears to be bounded by a rather sharp NE-SW elongated region marked by higher resistivity (Figure 3f). Such direction corresponds to the strike of Watukosek fault system. Several authors pointed out that the main piercements in the region (both magmatic and mud volcanoes) are aligned following the same direction of this fault system (Lupi et al., 2018; Mazzini et al., 2012; Miller & Mazzini, 2018). This structure becomes evident in the back-arc basin with a prominent fault escarpment (i.e., the Watukosek escarpment), a sudden kink of the Porong River, and laterally extensive fractures on the field (Mazzini et al., 2009; Sciarra et al., 2018). Our geoelectrical data are consistent with the gravimetric results from Mauri, Husein, Mazzini, Irawan, et al. (2018) and Osorio Riffo et al. (2021) in tracing a NE-striking structure (Watukosek fault). Vertical profiles (Figure 3a) show that, unlike most of the piercements, the shallow part of the Lusi conduit is not vertical but rather has a 30 dip westwards. Such dip was also pointed out by Mazzini et al., (2009) and Moscariello et al. (2018) for the portion of the Watukosek fault reaching the surface in the area upon which Lusi resides. On a broader scale, also Fallahi et al. (2017) observed a westward dipping of the low velocity anomaly corridor connecting Lusi and the neighboring Arjuno Welirang volcanic complex.

The presence of shallow antithetic structures that intersects Lusi with NW-SE direction has already been suggested by several authors based on field and geophysical observations (Mauri, Husein, Mazzini, Irawan, et al., 2018; Moscariello et al., 2018; Sciarra et al., 2018). Our inversion does not strongly highlight these antithetic structures, however it is possible to observe at shallow depths low resistivity regions extending towards both the east and the west, outside the embankment whose location is consistent with previous observations (Figures 1c–1d). We cannot exclude that the low resistivity areas observed (e.g., on the shallow horizontal profiles of Figure 1c) represent early stages of micro-basins resulting from the interaction between the Watukosek fault system and the antithetic faults. Indeed it exists a wealth of field evidence,

published or reported during PPLS daily reports (e.g., Mazzini, 2009; Obermann et al., 2018; Sciarra et al., 2018) documenting the formation of new fractures with NE-SW orientation (e.g., Watukosek fault system) or with E-W orientation (antithetic faults). The interaction between these systems generates at the surface tens of meters wide depressions and, in some cases it may result in meter scale mud breccia accretions. These may be interpreted as micro basins separated by compression zones where positive structures may arise. The corollary of this observation is that when Lusi pierced the Earth's surface in 2006, the boiling fluids trapped at depth capitalized on the enhanced hydraulic transmissivity of the Watukosek fault and migrated upwards exploiting the enhanced permeability of this fault structure. This is in agreement with models proposed by Mazzini et al. (2007, 2009, 2012) and Lupi et al. (2013) that suggested the central role of the Watukosek fault in promoting Lusi's inception. To the best of our knowledge this study represents the first 3D electrical tomographic image of an erupting mud-geysering hydrothermal vent. Lusi crops out in a densely populated region and the subsidence linked to the eruptive activity already caused several damages to the infrastructures. Future plans for hazard mitigation and risk reduction may focus on the Eastern side of the embankment where the hanging wall of the fault seems to occur.

4. Conclusions

We presented the 3D deep electrical resistivity tomography of the Lusi eruption site in East Java. The inverted data show a system dominated by a central conduit developing upon what we suggest being the trace of a branch of the Watukosek fault system. These findings provide valuable information to understand the processes that took place in older clastic eruptions driven by similar over pressure release mechanisms. Additionally, our data have relevant implications for the hazard mitigation of Lusi and helps guiding the engineering work carried out daily by the mitigation Ministry Agency (PPLS) to contain this natural disaster. Finally, our work has also an important scientific impact as it points out the intimate link between the Watukosek fault system, the propagation of deep-seated fluids in the back arc and ultimately to the birth of Lusi.

Data Availability Statement

All the data analyzed during this study are stored under the DOI: https://zenodo.org/search?page=1&size=20&q=5148381. We also would like to thank all the students who made the survey possible. PPLS colleagues are thanked for their support during the field operations. Finally, we thank the editor and the reviewers for their constructive comments that improved this manuscript.

Acknowledgments
The work was funded by the European Research Council under the European Union's Seventh Framework Program Grant agreement no 308126 (Lusi LAB project, PI A. Mazzini). We acknowledge the support of the Research Council of Norway (NFR) through the HOTMUD project number 288299 and its Centres of Excellence funding scheme, project number 223272 (CEED). Matteo Lupi is a SCCER-SoE Professor and thanks the KTI for financial help.

References

Alizadeh, A. A., Guliyev, I. S., Kadirov, F. A., & Eppelbaum, L. V. (2016). Mud Volcanism. In A. A. Alizadeh, I. S. Guliyev, F. A. Kadirov, & L. V. Eppelbaum (Eds.), Geosciences of Azerbaijan: Volume I Geology (Vol. Volume 1, pp. 215–233): Springer International Publishing. https://doi.org/10.1007/978-3-319-27395-2_7

Aoki, Y., & Sidiq, T. P. (2014). Ground deformation associated with the eruption of Lumpur Sidoarjo mud volcano, east Java, Indonesia. *Journal of Volcanology and Geothermal Research*, *278–279*, 96–102. https://doi.org/10.1016/j.jvolgeores.2014.04.012

Balasco, M., Galli, P., Giocoli, A., Gueguen, E., Lapenna, V., Perrone, A., et al. (2011). Deep Geophysical Electromagnetic Section Across The Middle 325 Aterno Valley (Central Italy): Preliminary Results After The April 6, 2009 L'aquila Earthquake: Bollettino 326 Di Geofisica Teorica Ed Applicata, 52(3), 443–455.

Berndt, C., Perez-Garcia, C., Planke, S., Mienert, J., & Bünz, S. (2006). The Plumbing system of the Håkon Mosby Mud Volcano - New insights from high-resolution 3D seismic data: AAPG/GSTT Hedberg Conference "Mobile Shale Basins - Genesis, Evolution and Hydrocarbon Systems". Port-of-Spain, Trinidad and Tobago, June 5-7, 2006.

Carrier, A., Fischanger, F., Gance, J., Cocchiararo, G., Morelli, G., & Lupi, M. (2019). Deep electrical resistivity tomography for the prospection of low- to medium-enthalpy geothermal resources. *Geophysical Journal International*, *219*(3), 2056–2072. https://doi.org/10.1093/gji/ggz411

Collignon, M., Mazzini, A., Schmid, D. W., & Lupi, M. (2018). Modelling fluid flow in active clastic piercements: Challenges and approaches. *Marine and Petroleum Geology*, *90*, 157–172. https://doi.org/10.1016/j.marpetgeo.2017.09.033

Collignon, M., Schmid, D. W., Galerne, C., Lupi, M., & Mazzini, A. (2018). Modelling fluid flow in clastic eruptions: Application to the Lusi mud eruption. *Marine and Petroleum Geology*, *90*, 173–190. https://doi.org/10.1016/j.marpetgeo.2017.08.011

Credit Crisp. (2005). https://crisp.nus.edu.sg/

Deville, E., Battani, A., Griboulard, R., Guerlais, S. H., Herbin, J. P., Houzay, J. P., et al. (2003). Mud volcanism origin and processes. New insights from Trinidad and the Barbados Prism. In P. Van Rensbergen, R. R. Hillis, A. J. Maltman, & C. Morley (Eds.), Surface Sediment Mobilization (Vol. 216, pp. 475–490): Special publication of the Geological Society (London). https://doi.org/10.1144/gsl.sp.2003.216.01.31

Deville, É., Guerlais, S.-H., Lallemant, S., & Schneider, F. (2010). Fluid dynamics and subsurface sediment mobilization processes: An overview from Southeast Caribbean: Fluid dynamics and subsurface sediment mobilization processes. *Basin Research*, *22*(4), 361–379. https://doi.org/10.1111/j.1365-2117.2010.00474.x

Di Felice, F., Mazzini, A., Di Stefano, G., & Romeo, G. (2018). Drone high resolution infrared imaging of the Lusi mud eruption. *Marine and Petroleum Geology*, *90*, 38–51. https://doi.org/10.1016/j.marpetgeo.2017.10.025

Di Stefano, G., Romeo, G., Mazzini, A., Iarocci, A., Hadi, S., & Pelphrey, S. (2018). The Lusi drone: A multidisciplinary tool to access extreme environments. *Marine and Petroleum Geology*, *90*, 26–37. https://doi.org/10.1016/j.marpetgeo.2017.07.006

Dupuis, M., Imbert, P., Odonne, F., & Vendeville, B. (2019). Mud volcanism by repeated roof collapse: 3D architecture and evolution of a mud volcano cluster offshore Nigeria. *Marine and Petroleum Geology*, *110*, 368–387. https://doi.org/10.1016/j.marpetgeo.2019.07.033

Fallahi, M. J., Obermann, A., Lupi, M., Karyono, K., & Mazzini, A. (2017). The Plumbing system feeding the Lusi eruption revealed by ambient noise tomography. *Journal of Geophysical Research-Solid Earth*, *122*(10), 8200–8213. https://doi.org/10.1002/2017jb014592

Fukushima, Y., Mori, J., Hashimoto, M., & Kano, Y. (2009). Subsidence associated with the LUSI mud eruption, East Java, investigated by SAR interferometry. *Marine and Petroleum Geology*, *26*, 1740–1750. https://doi.org/10.1016/j.marpetgeo.2009.02.001

Gudmundsson, M. T., Thordarson, T., Höskuldsson, Á., Larsen, G., Björnsson, H., Prata, F. J., et al. (2012). Ash generation and distribution from the April-May 2010 eruption of Eyjafjallajökull, Iceland, *Scientific Reports*, *2*(1), 572. https://doi.org/10.1038/srep00572

Günther, T., Rücker, C., & Spitzer, K. (2006). Three-dimensional modelling and inversion of dc resistivity data incorporating topography-II. Inversion. *Geophysical Journal International*, *166*(2), 506–517. https://doi.org/10.1111/j.1365-246x.2006.03011.x

Inguaggiato, S., Mazzini, A., Vita, F., & Sciarra, A. (2018). The Arjuno-Welirang volcanic complex and the connected Lusi system: Geochemical evidences. *Marine and Petroleum Geology*, *90*, 67–76. https://doi.org/10.1016/j.marpetgeo.2017.10.015

Istadi, B. P., Pramono, G. H., Sumintadireja, P., & Alam, S. (2009). Modeling study of growth and potential geohazard for LUSI mud volcano: East Java, Indonesia. *Marine and Petroleum Geology*, *26*(9), 1724–1739. https://doi.org/10.1016/j.marpetgeo.2009.03.006

Karyono, K., Obermann, A., Lupi, M., Masturyono, M., Hadi, S., Syafri, I., et al. (2017). Lusi, a clastic-dominated geysering system in Indonesia recently explored by surface and subsurface observations. *Terra Nova*, *29*(1), 13–19. https://doi.org/10.1111/ter.12239

Kirkham, C., Cartwright, J., Hermanrud, C., & Jebsen, C. (2017). The spatial, temporal and volumetric analysis of a large mud volcano province within the Eastern Mediterranean. *Marine and Petroleum Geology*, *81*, 1–16. https://doi.org/10.1016/j.marpetgeo.2016.12.026

Kopf, A. J. (2008). Making calderas from mud. *Nature Geoscience*, *1*(8), 500–501. https://doi.org/10.1038/ngeo256

Lajaunie, M., Gance, J., Nevers, P., Malet, J. P., Bertrand, C., Garin, T., & Ferhat, G. (2019). Structure of the Séchilienne unstable slope from large-scale three-dimensional electrical tomography using a Resistivity Distributed Automated System (R-DAS). *Geophysical Journal International*, *219*(1), 129–147. https://doi.org/10.1093/gji/ggz259

Lupi, M., Mazzini, A., Sciarra, A., Collignon, M., Schmid, D. W., Husein, A., et al. (2018). Enhanced hydrothermal processes at the new-born Lusi eruptive system, Indonesia. *Journal of Volcanology and Geothermal Research*, *366*, 47–57. https://doi.org/10.1016/j.jvolgeores.2018.09.006

Lupi, M., Saenger, E. H., Fuchs, F., & Miller, S. A. (2013). Lusi mud eruption triggered by geometric focusing of seismic waves. *Nature Geoscience*, *6*(8), 642–646. https://doi.org/10.1038/ngeo1884

Lupi, M., Saenger, E. H., Fuchs, F., & Miller, S. A. (2014). Corrigendum: Lusi mud eruption triggered by geometric focusing of seismic waves. *Nature Geoscience*, *7*(9), 687–688. https://doi.org/10.1038/ngeo2239

Malvoisin, B., Mazzini, A., & Miller, S. A. (2018). Deep hydrothermal activity driving the Lusi mud eruption. *Earth and Planetary Science Letters*, *497*, 42–49. https://doi.org/10.1016/j.epsl.2018.06.006

Mauri, G., Husein, A., Mazzini, A., Irawan, D., Sohrabi, R., Hadi, S., et al. (2018). Insights on the structure of Lusi mud edifice from land gravity data. *Marine and Petroleum Geology*, *90*, 104–115. https://doi.org/10.1016/j.marpetgeo.2017.05.041

Mauri, G., Husein, A., Mazzini, A., Karyono, K., Obermann, A., Bertrand, G., et al. (2018). Constraints on density changes in the funnel-shaped caldera inferred from gravity monitoring of the Lusi mud eruption. *Marine and Petroleum Geology*, *90*, 91–103. https://doi.org/10.1016/j.marpetgeo.2017.06.030

Mazzini, A. (2009). Mud volcanism: Processes and implications. *Marine and Petroleum Geology*, *26*(9), 1677–1680. https://doi.org/10.1016/j.marpetgeo.2009.05.003

Mazzini, A., & Etiope, G. (2017). Mud volcanism: An updated review. *Earth-Science Reviews*, *168*, 81–112. https://doi.org/10.1016/j.earscirev.2017.03.001

Mazzini, A., Etiope, G., & Svensen, H. (2012). A new hydrothermal scenario for the 2006 Lusi eruption, IndonesiaInsights from gas geochemistry. *Earth and Planetary Science Letters*, *317*, 305–318. https://doi.org/10.1016/j.epsl.2011.11.016

Mazzini, A., Lupi, M., Sciarra, A., Hammed, M., Schmidt, S. T., & Suessenberger, A. (2019). Concentric structures and hydrothermal venting in the Western Desert, Egypt. *Frontiers in Earth Science*, *7*–266. https://doi.org/10.3389/feart.2019.00266

Mazzini, A., Nermoen, A., Krotkiewski, M., Podladchikov, Y., Planke, S., & Svensen, H. (2009). Strike-slip faulting as a trigger mechanism for overpressure release through piercement structures. Implications for the Lusi mud volcano, Indonesia. *Marine and Petroleum Geology*, *26*(9), 1751–1765. https://doi.org/10.1016/j.marpetgeo.2009.03.001

Mazzini, A., Scholz, F., Svensen, H. H., Hensen, C., & Hadi, S. (2018). The geochemistry and origin of the hydrothermal water erupted at Lusi, Indonesia. *Marine and Petroleum Geology*, *90*, 52–66. https://doi.org/10.1016/j.marpetgeo.2017.06.018

Mazzini, A., Sciarra, A., Etiope, G., Sadavarte, P., Houweling, S., Pandey, S., & Husein, A. (2021). Relevant methane emission to the atmosphere from a geological gas manifestation. *Scientific Reports*, *11*(1), 4138. https://doi.org/10.1038/s41598-021-83369-9

Mazzini, A., Svensen, H., Akhmanov, G. G., Aloisi, G., Planke, S., Malthe-Sorenssen, A., & Istadi, B. (2007). Triggering and dynamic evolution of the LUSI mud volcano, Indonesia. *Earth and Planetary Science Letters*, *261*(3–4), 375–388. https://doi.org/10.1016/j.epsl.2007.07.001

Miller, S. A., & Mazzini, A. (2018). More than ten years of Lusi: A review of facts, coincidences, and past and future studies. *Marine and Petroleum Geology*, *90*, 10–25. https://doi.org/10.1016/j.marpetgeo.2017.06.019

Moscariello, A., Do Couto, D., Mondino, F., Booth, J., Lupi, M., & Mazzini, A. (2018). Genesis and evolution of the Watukosek fault system in the Lusi area (East Java). *Marine and Petroleum Geology*, *90*, 125–137. https://doi.org/10.1016/j.marpetgeo.2017.09.032

Obermann, A., Karyono, K., Diehl, T., Lupi, M., & Mazzini, A. (2018). Seismicity at Lusi and the adjacent volcanic complex, Java, Indonesia. *Marine and Petroleum Geology*, *90*, 149–156. https://doi.org/10.1016/j.marpetgeo.2017.07.033

Osorio Riffo, Á., Mauri, G., Mazzini, A., & Miller, S. A. (2021). Tectonic insight and 3-D modelling of the Lusi (Java, Indonesia) mud edifice through gravity analyses. *Geophysical Journal International*, *225*(2), 984–997. https://doi.org/10.1093/gji/ggab020

Panzera, F., D'Amico, S., Lupi, M., Mauri, G., Karyono, K., & Mazzini, A. (2018). Lusi hydrothermal structure inferred through ambient vibration measurements. *Marine and Petroleum Geology*, *90*, 116–124. https://doi.org/10.1016/j.marpetgeo.2017.06.017

Planke, S., Rassmussen, T., Rey, S. S., & Myklebust, R. (2005). Seismic characteristics and distribution of volcanic intrusions and hydrothermal vent complexes in the Vøring and Møre basins: Petroleum Geology: North-West Europe and Global Perspectives: Proceedings of the 6th Petroleum Geology Conference, p. 833-844. https://doi.org/10.1144/0060833

Planke, S., Svensen, H., Hovland, M., Banks, D., & Jamtveit, B. (2003). Mud and fluid migration in active mud volcanoes in Azerbaijan. *Geo-Marine Letters*, *23*, 258–268. https://doi.org/10.1007/s00367-003-0152-z

Praeg, D., Ceramicola, S., Barbieri, R., Unnithan, V., & Wardell, N. (2009). Tectonically-driven mud volcanism since the late Pliocene on the Calabrian accretionary prism, central Mediterranean Sea. *Marine and Petroleum Geology*, *26*(9), 1849–1865. https://doi.org/10.1016/j.marpetgeo.2009.03.008

Pucci, S., Civico, R., Villani, F., Ricci, T., Delcher, E., Finizola, A., et al. (2016). Deep electrical resistivity tomography along the tectonically active Middle Aterno Valley (2009 L'Aquila earthquake area, central Italy). *Geophysical Journal International*, *207*(2), 967–982. https://doi.org/10.1093/gji/ggw308

Revil, A., Finizola, A., Ricci, T., Delcher, E., Peltier, A., Barde-Cabusson, S., et al. (2011). Hydrogeology of Stromboli volcano, Aeolian Islands (Italy) from the interpretation of resistivity tomograms, self-potential, soil temperature and soil CO_2 concentration measurements. *Geophysical Journal International*, *186*(3), 1078–1094. https://doi.org/10.1111/j.1365-246x.2011.05112.x

Rücker, C., Günther, T., & Spitzer, K. (2006). Three-dimensional modelling and inversion of dc resistivity data incorporating topography–I. Modelling. *Geophysical Journal International*, *166*(2), 495–505. https://doi.org/10.1111/j.1365-246x.2006.03010.x

Rudolph, M. L., Shirzaei, M., Manga, M., & Fukushima, Y. (2013). Evolution and future of the Lusi mud eruption inferred from ground deformation. *Geophysical Research Letters*, *40*(6), 1089–1092. https://doi.org/10.1002/grl.50189

Samankassou, E., Mazzini, A., Chiaradia, M., Spezzaferri, S., Moscariello, A., & Do Couto, D. (2018). Origin and age of carbonate clasts from the Lusi eruption, Java, Indonesia. *Marine and Petroleum Geology*, *90*, 138–148. https://doi.org/10.1016/j.marpetgeo.2017.11.012

Sciarra, A., Mazzini, A., Inguaggiato, S., Vita, F., Lupi, M., & Hadi, S. (2018). Radon and carbon gas anomalies along the Watukosek Fault System and Lusi mud eruption, Indonesia. *Marine and Petroleum Geology*, *90*, 77–90. https://doi.org/10.1016/j.marpetgeo.2017.09.031

Shirzaei, M., Rudolph, M. L., & Manga, M. (2015). Deep and shallow sources for the Lusi mud eruption revealed by surface deformation. *Geophysical Research Letters*, *42*(13), 5274–5281. https://doi.org/10.1002/2015gl064576

Svensen, H., Jamtveit, B., Planke, S., & Chevallier, L. (2006). Structure and evolution of hydrothermal vent complexes in the Karoo Basin, South Africa. *Journal of the Geological Society*, *163*, 671–682. https://doi.org/10.1144/1144-764905-037

Svensen, H. H., Iyer, K., Schmid, D. W., & Mazzini, A. (2018). Modelling of gas generation following emplacement of an igneous sill below Lusi, East Java, Indonesia. *Marine and Petroleum Geology*, *90*, 201–208. https://doi.org/10.1016/j.marpetgeo.2017.07.007

Troiano, A., Isaia, R., Di Giuseppe, M. G., Tramparulo, F. D. A., & Vitale, S. (2019). Publisher correction: Deep electrical resistivity tomography for a 3D picture of the most active sector of Campi Flegrei caldera. *Scientific Reports*, *9*(1), 20308. https://doi.org/10.1038/s41598-019-55791-7

Van Noorden, R. (2006). Mud volcano floods Java. *Nature*. https://doi.org/10.1038/news060828-1

Zaputlyaeva, A., Mazzini, A., Blumenberg, M., Scheeder, G., Kürschner, W. M., Kus, J., et al. (2020). Recent magmatism drives hydrocarbon generation in north-east Java, Indonesia. *Scientific Reports*, *10*(1), 1786. https://doi.org/10.1038/s41598-020-58567-6

Zaputlyaeva, A., Mazzini, A., Caracausi, A., & Sciarra, A. (2019). Mantle-derived fluids in the East Java Sedimentary Basin, Indonesia. *Journal of Geophysical Research: Solid Earth*, *124*(8), 7962–7977. https://doi.org/10.1029/2018jb017274